RESEARCH ARTICLE

Comparative immunohistochemical and ultrastructural study on the developing autopod of the toad *Bufo regularis* and the chick *Gallus domesticus*

Gamal M. Badawy*, Saber A. Sakr, and Marwa M. Attalah
Department of Zoology, Faculty of Science, Menoufiya University, Egypt

Manuscript Info

*Corresponding Author
Gamal M. Badawy
Gamalbadawy940@yahoo.com

Abstract

The present study has dealt with investigating certain morphogenetic aspects of the developing limb autopod in two different tetrapod models, namely, the toad *Bufo regularis* and the chick *Gallus domesticus*. One of the aims was to examine whether or not the amphibian model under consideration displays interdigital programmed cell death (IPCD) and if not, try to find the alternative way by which morphogenetic process of the limb autopod occurs. This has been attempted using standard immunohistochemical technique and employing caspase-3. Based on the negative results emerged from the latter approach in case of the toad, immunohistochemical evaluation of cellular proliferation using proliferating cell nuclear antigen (PCNA) has been carried out. The results showed that the IPCD is an integral part of the formation of free digits in the chick embryo, while it is never a part of free digit formation in the developing toad. In the latter, cell migration and differential growth are the alternative processes through which digits can be formed. Ultrastructurally, IPCD was accompanied by a high deposition of collagenous material in the epithelial-mesenchyme interface, rupture of the basal lamina and detachment of ectodermal cells. Most interdigital dying cells appeared rounded and electron dense with the nucleus exhibiting a characteristic peripheral condensation of the chromatin accompanied with vacuolation of most of the cytoplasmic organelles and the appearance of lysosomes. Macrophages appeared gradually in the mesoderm to eliminate cellular debris. The mitochondria of the interdigital area appeared distorted and this referred to the intrinsic pathway of caspase action.

Introduction

Among the basic cellular activities, programmed cell death (PCD) is involved in the control of a variety of biologically important processes especially developmental morphogenesis. It participates in the regulation of the number of cells in the different tissues and contributes to sculpturing the shape of many developing structures (Merino *et al*., 1999). Consequently, PCD is now recognized as a key factor in embryonic development (Maghsoudi *et al*., 2012). The developing vertebrate limb illustrates particularly well how correct morphogenesis depends on the appropriate spatial and temporal balance between PCD and cell proliferation, the paradigm being the separation of the digits (Shou *et al.,* 2013). Precise knowledge of the patterns of cell proliferation and PCD during limb development is required to understand how their modifications may contribute to the generation of the great diversity of limb phenotypes among vertebrates. Individualization of the digits is then progressively achieved partly through the morphogenetic role of removal of the interdigital tissue by PCD (Saunders *et al*., 1962; Hinchliffe, 1982).

Interdigital programmed cell death (IPCD) is a morphogenetic event that has been proposed to be essential for tissue modeling and digit separation during limb formation in amniotes (Jacobson *et al*., 1997; Shou *et al.,* 2013). It was first discovered as massive cell degeneration in the interdigital mesoderm using avian embryo (Saunders and Fallon, 1966) and thereafter a concept was established that the morphogenetic roles of IPCD are in causing separation of digits through shaping and remodeling the contours of the digital plate (Hinchliffe and Thorogood, 1974). Massive PCD in the mesenchyme of the interdigital areas accompanies the formation of free digits in reptiles (Fallon and Cameron, 1977), birds **(**Fernández-Terán *et al*., 2006**),** and mammals (Milaire, 1977; Salas-Vidal *et al*., 2001**).** In all mentioned animal classes the digits primarily differentiate from the mesenchyme of the fan-shaped hand or foot plate where prechondrogenic condensations are the first sign of the thickened digital rays separated by the flattened interdigital tissue. This will determine the different outcome of cells in both regions, since condensations will progress to make cartilage, whereas interdigital cells ultimately will either die by IPCD *i.e.,* apoptosis or migrate **(**Chen and Zhao, 1998; Sato *et al*., 2010).

It is now generally accepted that the digits of most vertebrates develop by detaching from an initial hand or foot plate. The mechanism of digit detachment has received considerable attention from embryologists and IPCD has been widely accepted as the main factor involved in the process and its failure, either genetically or with drug-induced inhibition of IPCD, leads to soft tissue syndactyly, a generic name given to limbs with joined digits (Hinchliffe and Thorogood, 1974; Hinchliffe, 1982; Hernández-Martínez and Covarrubias, 2011**).** The mechanisms involved in setting up the digital versus interdigital areas and thus spacing the digits are not fully understood. The initial divergence between the digital and interdigital areas determines the fate of cells in an alternating fashion, and different programmes of cell differentiation (chondrogenesis or apoptosis, respectively) will be activated accordingly. Later in limb development, during the period of digit formation in the autopod, the cells located in the interdigital areas undergo PCD and serve the function of sculpturing the shape of the digits **(**Hurlé *et al*., 1996**).** In the chick limb, dying cells in the interdigits first appear as a cluster in the proximal mesenchyme, and subsequently, a second apoptotic cell cluster is detected in the distal mesenchyme. As development progresses, both clusters connect together to form a common domain of IPCD area (Fernández-Terán *et al*., 2006).

Caspases are of central importance in the apoptotic signaling network which is activated in most cases of apoptotic PCD (Bratton *et al*., 2000). The term caspases is derived from cysteine-dependent aspartate-specific proteases. Caspases are widely expressed in an inactive proenzyme form in most cells and once activated can often activate other pro-caspases, allowing initiation of a protease cascade. This proteolytic cascade, in which one caspase can activate other caspases, amplifies the apoptotic signaling pathway and thus leads to rapid cell death. Caspases have proteolytic activity and are able to cleave proteins at aspartic acid residues, although different caspases have different specificities involving recognition of neighboring amino acids. Once caspases are initially activated, there seems to be an irreversible commitment towards PCD (Elmore, 2007). Different studies have established that IPCD occurs through a caspase-dependent apoptotic process (Milligan *et al*., 1995; Jacobson *et al*., 1997) and in particular caspase-3 activity has been identified in the regressing interdigits (Umpierre *et al.,* 2001; Huang and Hales, 2002**).**

The use of immunohistochemical assays, based on antibodies to cell proliferation-related antigens, has proved to be effective in the assessment of cell proliferation **(**Kurki *et al***.,** 1988). One such cell proliferation-related protein is proliferating cell nuclear antigen (PCNA), which is found in the nuclei of proliferating cells and is therefore commonly considered as one of the proliferation markers. PCNA-labeling has become a faster and easier method to use for the detection of cell proliferation **(**Van Dierendonck *et al*., 1991). In addition, because the PCNA method is based on an antigen–antibody reaction, it can be performed *in situ*, on routinely processed tissue sections and its presence subsequent to immunohistochemical processing can be observed microscopically. This technique can be used for the purpose of providing direct visual evidence of cell proliferation under various experimental conditions (Tousson *et al*., 2011).

The morphogenesis of free digits cannot be adequately explained without an extensive analysis of the tissue changes taking place during the morphogenetic process and thus the ultrastructural study of the developing limb is crucial in order to understand the characteristics of cellular changes in the developing limb. Transmission electron microscopy studies have shown that cell death in the interdigital mesoderm follows a morphological pattern of apoptosis (García-Martinez *et al*., 1993; Mori *et al*., 1995). Dying cells exhibit both nuclear and cytoplasmic alterations detectable by light, transmission, and scanning electron microscopy (reviewed in Hurlé *et al*., 1996). The apoptotic cells undergo fragmentation and the fragments resulting from this process appear as darkly stained spherules which usually contain a small nuclear fragment. The resulting debris is removed by phagocytosis (Steller, 1995). The origin of phagocytes has been debated, however, it is now accepted that phagocytosis is performed both by the neighboring healthy mesenchyme cells and by incoming macrophages of hematopoietic origin (Hurlé *et al*., 1996; Montero and Hurlé, 2010).

The aims of this two-fold integrated study were firstly to investigate the unknown morphogenetic aspects of limb autopod in the toad *Bufo regularis*. The presence of limited IPCD within the developing limb of the seepage salamander (Franssen *et al.,* 2005) called for more investigation within other amphibian species. The amphibian model under consideration was thus subjected to investigation to see if its developing autopod displays IPCD and if not, try to find the alternative way by which morphogenetic process of the autopod occurs. Secondly, to describe the ultrastructural characters of the main cellular changes in the developing autopod of the chick *Gallus domesticus* using transmission electron microscopy. Although some aspects of their biology are understood, ultrastructural studies of avian limb development are evidently scarce.

MATERIALS and METHODS

Animals and care

All the experimental aspects of this work were conducted in compliance with the institutional guidelines for the care and use of animals. Two, amphibian and avian experimental models, namely, the tadpole *Bufo regularis* and the chick *Gallus domesticus* were utilized as representatives for tetrapods. For obtaining tadpoles, several ribbons of fertilized eggs of the toad, *Bufo regularis* were brought into the laboratory from the fields of Shebeen El-Koom districts during the breeding season which lasts from March to September. Developing eggs were collected in a mesh-collecting basket and shipped in plastic bags filled with de-chlorinated tap water. The ribbons were divided into small bunches and kept in white enamel-coated pans provided with two liters of de-chlorinated tap water. Tadpoles were fed *ad libitum* either freshly or frozen boiled spinach and rearing water was changed every necessitation that was at least once weekly. Rearing took place at room temperature that was 28 ± 2 ˚C. Based on our previous investigation (Badawy *et al.,* 2012), four developmental stages were selected *i.e.,* 53, 54, 55 and 56 according to the normal table of Sedra and Michael (1961).

Normal fertilized hen eggs, of a local strain were obtained from a local breeder at Shebeen El-Koom, Menoufiya governorate. Before incubation at 37˚C in an artificial incubator, eggs were cleaned with distilled water followed by 70% ethanol. To ensure the relevant humidity (65%), an open 1-liter container filled with distilled water was placed at the bottom of the incubator. The eggs were put horizontally and turned over, at least, three times a day. Based on our previous investigation (Badawy *et al.,* 2012), four developmental stages were selected *i.e.,* 30, 31, 32 and 33 according to the normal table of Hamburger and Hamilton (1951).

Sampling and manipulation of tadpole autopods

As the fore limb was still concealed by the skin of the operculum at the four investigated developmental stages, it was isolated using dissecting binocular microscope and following the method mentioned in our previous investigation (Badawy *et al.,* 2012). Limbs were fixed in 10 % formalin for 24 hours, washed under running tap water for 12 hours and then stored in 70 % ethanol until further

processing. For obtaining semithin sections, the autopods were fixed in Karnovsky's fixative (pH 7.4). A total number of 240 tadpoles was utilized during the investigation.

Sampling and manipulation of chick embryo autopods

At the appropriate times for staging according to the normal table of Hamburger and Hamilton (1951), eggs were windowed following the protocol of Korn and Cramer (2007). The albumen and yolk were then poured off and the chick embryo was taken out of the egg into a Petri dish and washed several times with avian saline (0.75 % NaCl). The extra-embryonic membranes were carefully removed in order to have free access to the limbs. Chick embryos of the investigated developmental stages were anesthetized wholly in ether for 30 minutes and then moved to 10 % formalin for an hour. For each stage, ten embryos were sacrificed and the limbs were fixed in 10 % formalin for 24 hours, washed under running tap water for 12 hours and then stored in 70 % ethanol until the start of the immunohistochemical investigation. Another five embryos per each developmental stage were sacrificed and the autopods were fixed in Karnovsky's fixative (pH 7.4) for ultrastructural investigation. A total of 60 chick embryos were utilized.

A- Immunohistochemical investigation

In order to identify the possible apoptotic cells in the developing tadpole and chick autopods, immunohistochemical technique employing caspase-3 as an indicator for the occurrence of apoptosis was adopted. Expression of caspase protein was therefore detected using Avidin biotin complex (ABC) immunohistochemical method (Sternberger, 1979).

For this purpose the following steps were performed:

1- Samples of the autopods of both fore and hind limbs of the tadpole stages from 53 to 56 and chick developmental stages from 30 to 33 were fixed in 10 % formalin for 24 hours, washed under running tap water for 12 hours, then transferred to 70 % ethanol.

2- The samples were stained *in toto* in hematoxylin for 10 minutes, and transferred to 70 % ethanol, in order to determine the appropriate sections which assumed to reflect the possible apoptotic events for processing.

3- The samples were dehydrated in an ascending series of ethanol *i.e.,* 80 %, 90 %, 100 % I and 100 % II, 30 minutes each except the last change where the samples were kept for two hours. The samples were then cleared and embedded. Five μm thick serial longitudinal sections were produced and mounted on positive charged slides.

4- To reduce non-specific background staining due to endogenous peroxidase activity, the dewaxed and rehydrated sections were washed in phosphate buffered saline (PBS) for 5 minutes and treated with 0.3% H_2O_2 in methanol for 30 minutes.

5- Sections were washed with PBS for 15 minutes and incubated with blocking solution *i.e.,* 1.5 % normal goat serum in PBS.

6- Sections were incubated for 45 minutes with rabbit poly-clonal antihuman caspase-3 (0.5 mg/ml) in 1.5 % normal goat serum in PBS in moist chamber.

7- Sections were incubated with biotin-conjugated goat anti-rabbit for one hour at room temperature.

8- After washing with PBS, sections were further incubated with AB-Peroxidase complex (Nichirei, Tokyo, Japan) for one hour at room temperature followed by rinsing in PBS. The reaction was developed by using 20 mg 3.30-diaminobenzidine tetrahydrochloride (DAB, Wako pure chemical industries, Ltd) in 40 mL PBS, pH 7.2 containing 10 mL of hydrogen peroxide (H_2O_2) for 7–9 minutes at a dark room followed by washing with PBS and counterstained with hematoxylin for one minute, washed with tap water followed by PBS for 30 seconds.

9- Sections were then dehydrated through ascending grades of ethanol, cleared in xylol and coverslipped with DPX.

The criterion for a positive reaction confirming the presence of caspase-3 protein is a dark, brownish, intracytoplasmic precipitate. For the negative control, the primary antibody was omitted to guard against any false positive results that might develop from a non-specific reaction. Negative control sections were produced by substituting caspase-3 primary antibodies by normal goat serum. All stained slides were viewed using Olympus microscope and images were captured by a digital camera (Canon Power Shot A620). Brightness and contrast of the images were adjusted using Adobe Photoshop software (Adobe Systems, San Jose, CA).

For evaluation of cellular proliferation by PCNA detection in the autopods of the four selected tadpole developmental stages, the same immunohistochemical method was followed except for two main substantially differences. Firstly, an additional step was performed after step 5 where antigen retrieval was performed for 15 minutes using Biogenex Antigen Retrieval Citra solution in 90 °C water bath followed by allowing to cool for 20 minutes before continuing. Omission of this step resulted in either no significant staining or a profound decrease in staining intensity. Secondly, in step 6 sections were incubated overnight at 4°C in a humidified chamber with the primary antibody PCNA monoclonal mouse IgG (Oncogene Sciences, NY) at a concentration of 2 pg/ml in PBS.

PCNA-labeling index

This has been determined for the developing digital and interdigital areas by slide examination under the light microscope where the abundance of PCNA-positive nuclei was assessed by the ratio of the number of PCNA-positive nuclei (with brown nuclear staining) to the total number of nuclei (labeled and unlabeled) per unit area (0.002 mm^2) using square eye piece micrometer at a magnification of X400. Six sections from different specimens were analyzed at each developmental stage, and the mean values and standard error of the mean (SEM) were determined for both the digital and interdigital areas. Because of similarity, data obtained from investigating the fore limb autopods were only presented to avoid unnecessary repetition.

The labeling indices were determined by employing the following formulas:
Mean number of digital labeled cells / mean number of all digital cells for each digital area.
Mean number of interdigital labeled cells / mean number of all interdigital cells for each interdigital area.

B- Ultrastructural investigation

For ultrastructural investigation which has been done using the transmission electron microscope, the autopods were rapidly dissected from both the tadpole larvae (stages 53-56) (Sedra and Michael, 1961) and the chick embryos (stages 30-33) (Hamburger and Hamilton, 1951). These developmental stages were chosen because they reflect the period of digits formation. The dissected autopods were fixed rapidly for 4 hours at room temperature in Karnovsky fixative, (Karnovsky, 1965).

After rinsing in phosphate buffer, samples were post fixed in buffered solution of 1% osmium tetra-oxide for three hours at 4°C. The specimens were then washed in phosphate buffer several times for 10 minutes. This was followed by dehydration in ascending grades of ethanol and transferring to a solution of propylene oxide for clearing. The samples were then infiltrated in a mixture of propylene oxide and epon (1:1). After infiltration, tissues were embedded in the epoxy resins using beam capsules and blocks were prepared. Semithin sections of 1μm thickness stained with Toluidine blue were produced for light microscopical examination. Based on examining the semithin sections, the ultrastructural investigation was confined to the chick developmental stages.

After determining the desired areas from the semithin sections, ultra-thin (50 nm) sections were cut, mounted on formvar-coated grids and stained with uranyl acetate for 10 minutes. Sections were then stained with lead citrate for 10 minutes. Examination of grids was done by using JEOL electron microscope, Electron microscope unit, Tanta University, Tanta, Egypt. Selected sites were digitally photographed and then printed on Kodak sensitive printing paper.

Statistical analysis
        All data sets were expressed as mean ± SEM. The data were analyzed statistically for normal distribution (student's t test) and homogeneity of variances (Levene test) using SPSS software for windows, version 11. The significances of the obtained data were classified into three categories according to P values *i.e.,* $P<0.0001$, $P<0.03$ and $P<0.05$.

RESULTS

Immunohistochemical investigation
I- Caspase-3 immunoreactivity

A- Tadpole
         All sections taken from both fore and hind limb autopods of the tadpole developmental stages *i.e.*, 53, 54, 55 & 56 and subjected to caspase-3 primary antibodies, displayed negative immunoreaction as can be seen in Fig. 1 (A–F). This in turn indicated the absence of cell death in the developing tadpole autopod.

B- Chick
        The actual beginning of IPCD in the chick autopod, as expressed by applying caspase-3 immunohistochemical staining, started at stage 30 which represented the onset of reactivity. The apoptotic cells density increased with the advancement of the developmental stages. Fig. 2 (A&B) shows the apoptotic cells in the proximal part of the second (arrows) and third interdigital areas in the fore limb autopod of stage 30. More pronounced immunoreactive expression was evident at the developmental stage 31 (Fig. 2 C&D). The presence of macrophages was noticed in the interdigital area in Fig. 2 (C) (arrow heads).
        At the developmental stages 32 (Fig. 2 E–G) and 33 (Fig. 2 H&I), IPCD was massive and spread along the whole interdigital area of the fore limb autopod. By these stages, most of the interdigital tissue appeared to be immunostained. Wherever clusters of pyknotic nuclei were found, collections of macrophages were also present nearby (arrow heads). Many of these macrophages were very heavily laden with phagocytosed cellular material. Apoptotic debris could be seen in Fig. 2 (G), which resulted from discharge of macrophage digested contents.
        Similar to the fore limb investigation, IPCD was first detected at stage 30 in the proximal part of the hind limb interdigital mesenchyme (Fig. 3 A-C). Macrophages could also be identified in the epithelium (Fig. 3 B,C&F). Fig. 3 (D) shows that dead cells in the interdigital area first appeared as a cluster in the proximal mesenchyme, and subsequently, a second apoptotic cell cluster was detected in the distal mesenchyme of stage 31. Proximal and distal clusters of dead cells in the interdigital area of the same developmental stage later joined together and extended along the whole interdigital area (Fig. 3 E).
        The developmental stage 33 displayed an extensive increase in the IPCD which reached its peak. This resulted in the formation of interdigital spaces with apoptotic cells arranged along their peripheries and with apoptotic debris in the spaces itself as shown in Fig. 3 (G). The removal of the undifferentiated mesenchyme cells located between the developing digits caused the freeing of the digits from the foot plate. The epithelium also had macrophages discharging their contents to outside (Fig. 3 H).

II- PCNA- immunoreactivity

        Fig. 4 (A) shows cellular proliferation in the tadpole fore limb autopod of stage 53 where scattered labeled cells were uniformly distributed across the whole limb autopod. These immunoreactive proliferating cells were seen both in the epithelium and the underlying mesenchyme and resulted in an evident increase in the size and length of the developing autopod. After stage 53 there was an evident and

gradual decrease in the dividing cells especially in the interdigital area than in the digital area. Once the tips of the growing fingers protruded from the fore limb plate, the distal high level of cell proliferation was restricted to the digital tips, while the interdigital area had fewer mitotic cells (Fig. 4 B–D). Progressively, the chondrogenic skeletal elements displayed a clear decrease in proliferation in each central region, corresponding to the region where chondrocyte differentiation occurred. It was evident that the occurrence of dividing cells was high in early stages then decreased gradually in late ones.

The developing tadpole hind limb autopod showed similar results to that of the fore limb, though the density of the proliferating cells was high in the hind limb than in the fore limb. Mitoses were common both in the epithelium and the mesenchyme. These first became noticeable at stage 53 where the flattened extremity of the limb bud expanded to form the fully developed fan-shaped paddle (Fig. 4 E). As the condensation process started, mitotic activity decreased in the proximal mesenchyme of the autopod and began to show regional differences, however, the rate of cell division remained high in the epithelium and the distal mesenchyme at stage 54 (Fig. 4 F). The elongation and shovel-like expansion of the limb buds could therefore be explained by a more intense proliferation of mesenchyme in the distal region, compared to the proximal one. In the subsequent stages *i.e*., stage 55 (Fig. 4 G) and 56 (Fig. 4 H), there was a differential growth process of the autopod characterized by an intense growth of the digit tips and gradual decrease in the growth of the interdigital area. The density of the proliferating cells decreased gradually in the progressive developmental stages and became more restricted to the distal part of the autopod. The digital area had more dividing cells than the interdigital area.

Table (1) and Fig. (5) demonstrate differences in the percentage of PCNA labeled cells in both digital and interdigital areas of the fore limb autopod of the tadpole developmental stages 53, 54, 55 and 56.

Semithin sections of both toad and chick:

Before conducting the ultrastructural investigation, it was important to carefully investigate the semithin sections and treat them as a guide. The tadpole sections exhibited no signs for apoptosis as no apoptotic cells were detected within the whole range of the considered developmental stages (Fig. 7 A&B). However, chick developmental stages displayed evident signs of apoptosis in the autopod of both the fore limb (Fig. 7 C) and the hind limb (Fig. 7 D–F).

Ultrastructural investigation

The interdigital tissue analogue before stage 30 consisted of healthy mesenchyme cells lacking any signs of degeneration. As the present study is concerned with the way by which the morphogenesis of the limb autopod occurs, only the ultrastructural features of the interdigital area was considered. The epithelial layer of stage 30 was consisted of a basal layer of cuboidal cells covered by flattened peridermal cells rich in microfilaments (Fig. 7 A). The most significant feature of the epithelium at the ultrastructural level was the presence of abundant gap junctions and desmosomes (Fig. 7 A). This stage displayed the first signs of basal lamina discontinuities and the presence of collagen in the area of epithelial-mesenchyme interface. Within the mesenchyme of the interdigital area, there were few apoptotic cells and scarce macrophages with ingested dead cells in digestive vacuoles (Fig. 7 B).

At stage 31, the epithelial tissue of the interdigital area displayed clear regional differences in structure. The changes were present in both the mesenchyme and the epithelial tissues and especially in the epithelial-mesenchyme interface. Numerous apoptotic bodies (dead cell fragments) were in the course of being gradually phagocytosed by macrophages (referred as dc[1] i.e. recently ingested material, dc[2] i.e. partially digested material and dc[3] i.e. almost digested material was granular and pitted) (Fig. 7 C). At stage 32, bundles of microfilaments were abundant within the cytoplasm of both peridermal cells and basal cells (Fig. 7 D). The basal lamina discontinuities became more prominent than in the previous stage (Fig. 7 D and Fig. 8 B). The interdigital area showed an advanced stage of degeneration and the predominant feature was the presence of large macrophages containing numerous degenerated nuclei in their vacuoles (Fig. 8 A). Most mesenchyme cells were stellate with filopodia and contained well

236

developed organelles and some of them had lysosomes in their cytoplasm (Fig. 8 B). Within the mesenchyme, the number of macrophages and phagocytes engulfing pyknotic and degenerated nuclei increased compared with stage 31. The macrophages were larger with different stages of digested dead cells. (Fig. 8 A). Phagocytes were differentiated from macrophages in that they appeared as normal viable mesenchyme cells whose cytoplasm contained one or two dead cells (Fig. 8 B&C), however, macrophages contained many dead cells within well-defined digestive vacuoles. All the degenerated cells, as well as phagocytes and macrophages, tended to be located at the proximity of the epithelium, establishing in many instances close contacts with the ectodermal cells. The extracellular spaces at this stage were rich in collagen fibrils which were preferentially located in the most marginal zone of the interdigital area (Fig. 8 B&C). They were grouped into large clumps located between the mesenchyme cells and in the epithelial-mesenchyme interface. Later, mature macrophages with fully digested contents, found their way out to the amniotic sac through the epithelium (Fig. 8 B&C). The peridermal cells were characterized by the presence of abundant microvilli (Fig. 8C).

Fig. 8 (D–F) shows different isolated dead cells in the interdigital area of the fore limb of stage 33. These cells displayed different characteristic features of apoptosis. Apoptotic nuclei with characteristic peripheral condensation of the chromatin were abundant. Fragmented nucleus was also evident (Fig. 8 E). Most cell organelles were irregular like swollen mitochondria and dilated rough endoplasmic reticulum as well as dilated nuclear envelope and vacuolated cytoplasm (Fig. 8 F).

The ultrastructure of the interdigital area of the hind limb autopod was similar to that of the fore limb. Fig. 9 (A–D) shows the ultrastructure of the interdigital area at stage 30. The epithelium consisted of two layers, basal layer and peridermal layer with microvilli projecting into the amniotic sac (Fig. 9 A). Desmosomes and gap junctions were a characteristic feature of epithelial cells through which they were interconnected together (Fig. 9 A&B). The basal lamina was mostly continuous except at some regions along its length. Randomly distributed sublaminar collagen fibrils were also evident (Fig. 9 B). The mesenchyme just below the basal lamina in the neighboring digital area was condensed and showed a stable morphology with stellate mesenchyme cells with filopodia and small extracellular spaces (Fig. 9 C). However, some macrophages and degenerated nuclei during the process of phagocytosis were observed in the mesenchyme (Fig. 9 D). At stage 31, the basal lamina became more discontinuous (Fig. 9 E) accompanied with increased accumulation of sublaminar collagen fibrils. The number of macrophages increased with varying degree of ingested dead cells degradation (Fig. 9 F). A limited number of epithelium and mesenchyme cells showed well developed cell organelles, especially mitochondria and rough endoplasmic reticulum (Fig. 9 E, G & H). The discontinuities of the basal lamina were more prominent at stage 32 (Figs. 9 G&H and 10 A). The mesenchyme cells exhibited distorted organelles and chromatin condensation (Fig. 10 B). Different stages of macrophages were detected (Fig. 10 C).

Stage 33 displayed massive apoptotic figures and distorted cell organelles associated with an evident chromatin condensation (Fig. 10 D–H). Epithelium and mesenchyme cells contained many apoptotic cells with apoptotic nuclei which displayed peripheral chromatin condensation and lost cell borders. Distorted basal lamina was prominent (Fig. 10 E&H). Swollen mitochondria and dilated rough endoplasmic reticulum and nuclear envelope were evident (Fig. 10 F&G). A large number of degenerated phagocytes and macrophages were evidently observed in the mesenchyme (Fig. 10 G&H).
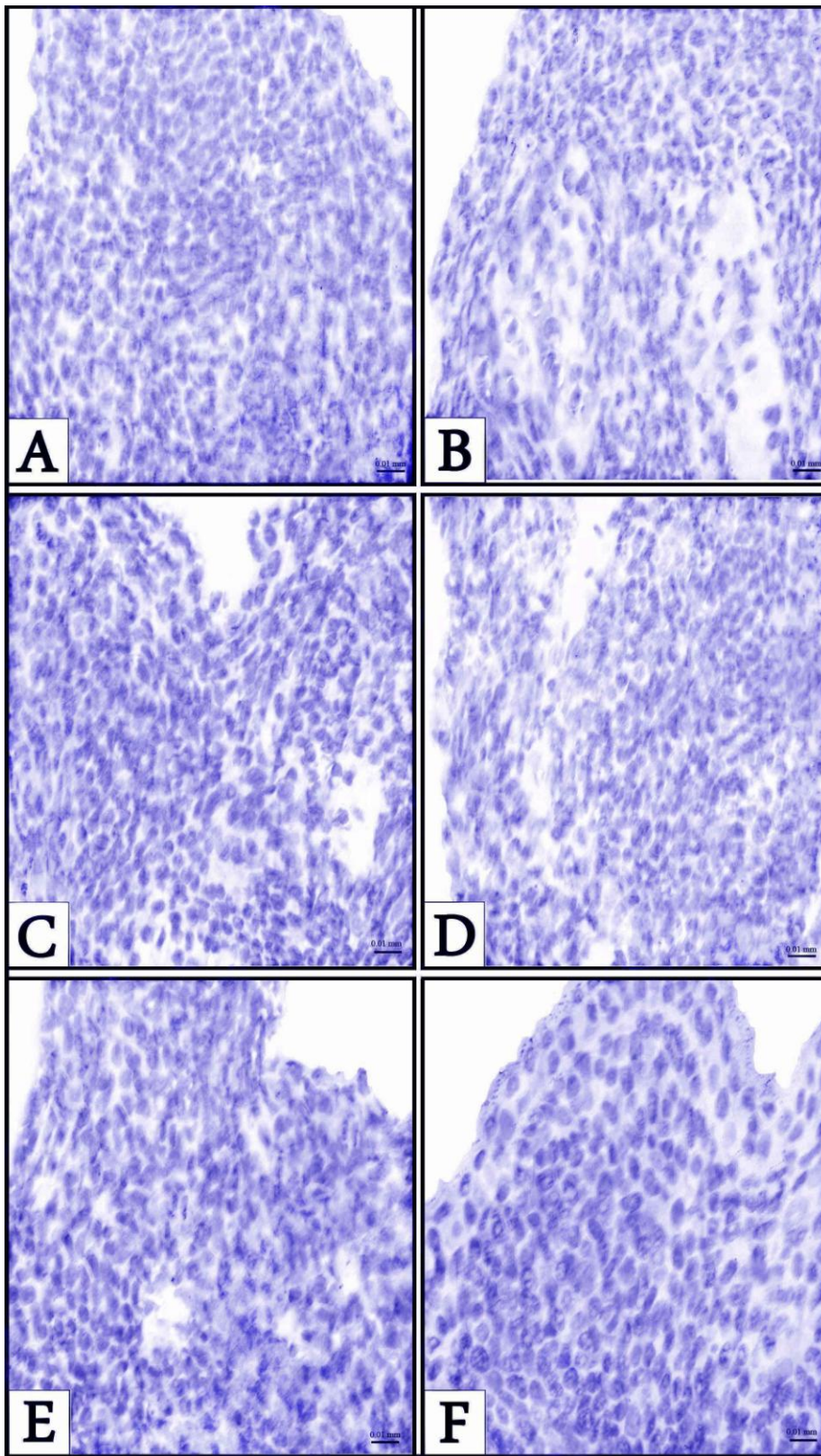
Fig. 1: Photomicrographs of representative Caspase-3 immunostained longitudinal sections through the   tadpole fore limb (A,B&C) and hind limb (D,E&F) autopods. Stages 53 (A&D), 55 (B&E) and 56 (C&F) showing the negative Caspase-3 immunoreaction. Scale bar = 0.01 mm.
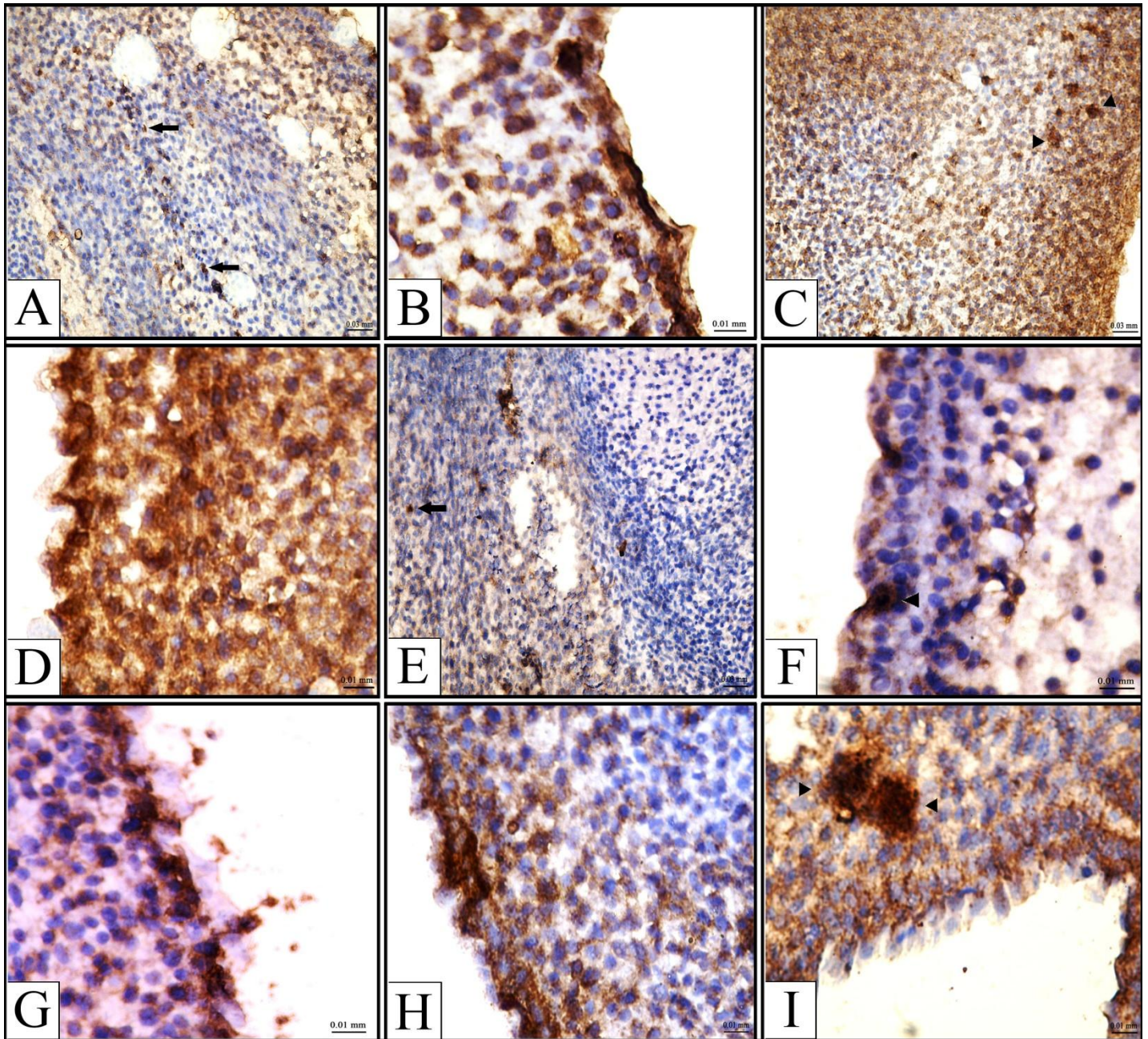
Fig. 2: Photomicrographs of representative Caspase-3 immunostained longitudinal sections through the chick fore limb autopods of stages 30 (A&B), 31 (C&D), 32 (E–G) and 33 (H&I) showing the pattern of cell death in the developing autopod. The brown-stained apoptotic cells were present in the interdigital area (arrows). Arrow heads indicate macrophages with ingested dead cells. Scale bar = 0.01 mm (B,D,G,H&I) and 0.03 mm (A,C&E).
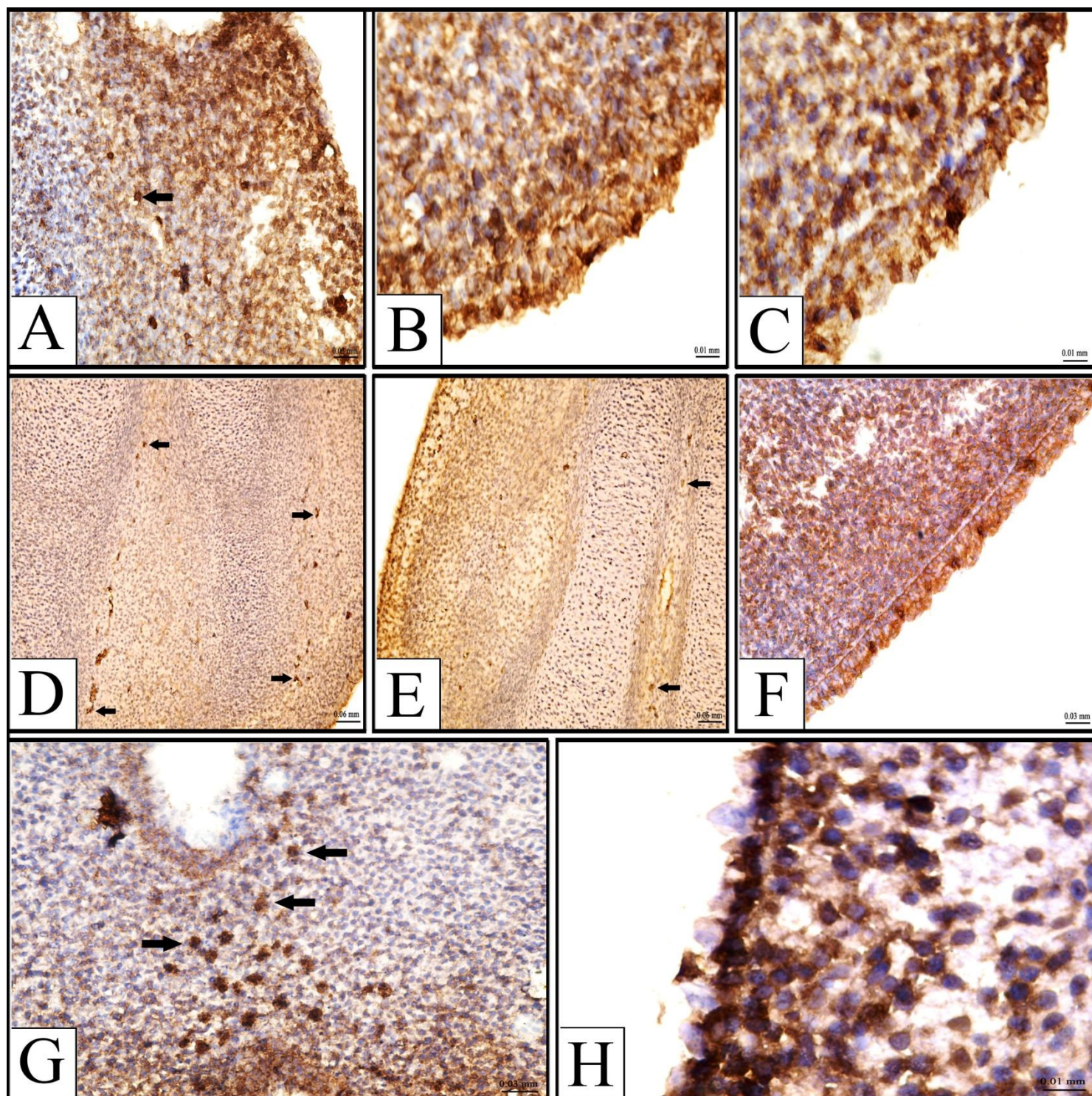
Fig. 3: Photomicrographs of representative Caspase-3 immunostained longitudinal sections through the chick hind limb autopods of stages 30 (A–C), 31 (D–F) and 33 (G&H). The apoptotic cells were scattered along the interdigital area. They first appeared as proximal and distal clusters (D) and then joined together at later stages (E) as indicated by the arrows. At stage 33, the macrophages and their ingested dead cells were present in the mesenchyme (G) and also in the epithelium (H). Scale bar = 0.03 mm (A,F&H), 0.01 mm (B,C&H) and 0.06 mm (D&E).
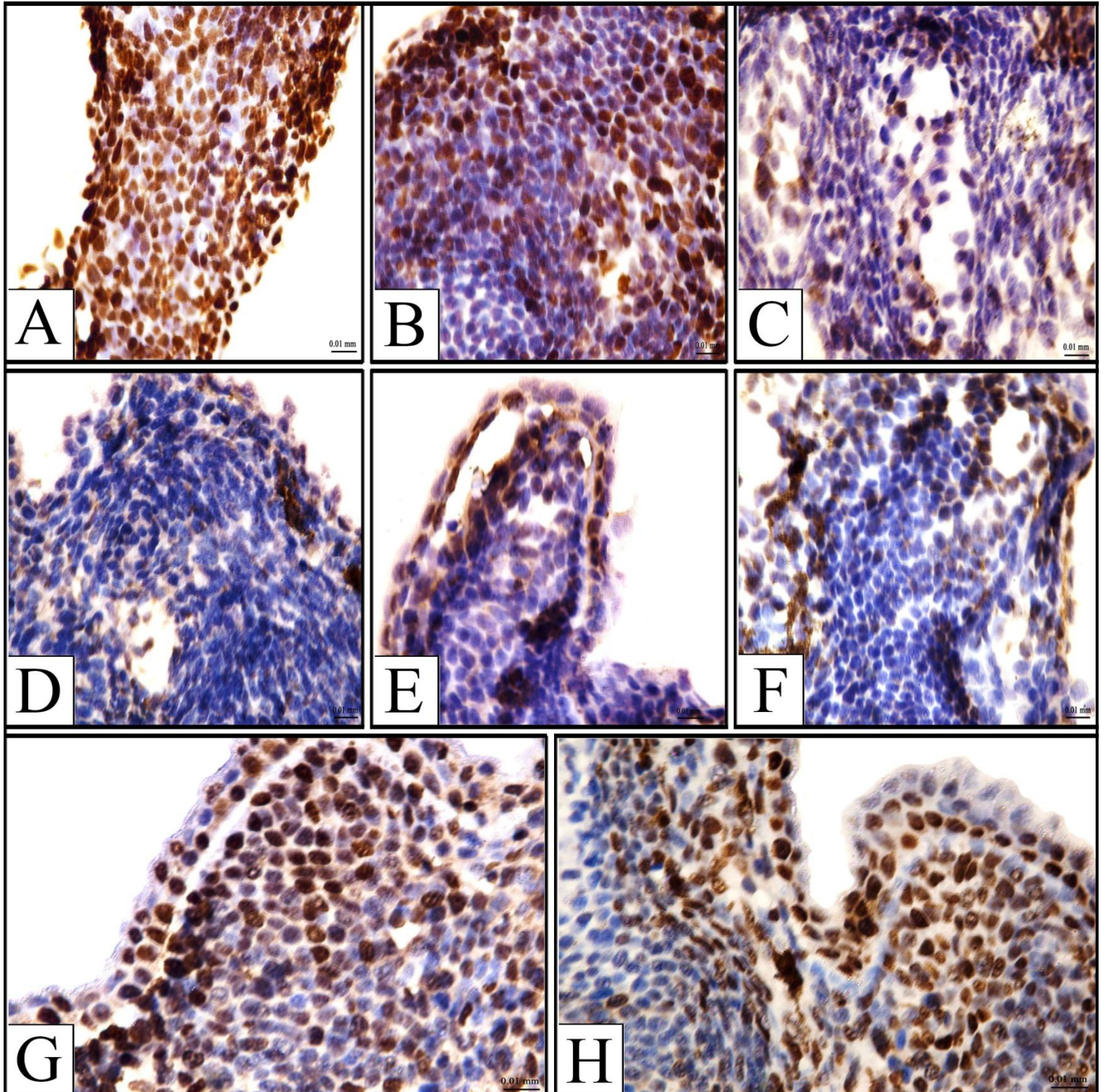
Fig. 4: Photomicrographs of representative PCNA immunostained longitudinal sections through the tadpole fore limb autopods of stages 53(A), 54 (B), 55 (C), 56 (D) and hind limb autopods of stages 53(E), 54 (F), 55 (G) and 56 (H) showing the pattern of cell proliferation in the developing autopod. The brown cells indicate PCNA labeled cells. Scale bar = 0.01 mm.

Developmental Stage	Area of Counting						
	D1	ID1	D2	ID2	D3	ID3	D4
53	94.60±0.58	86.20±1.03***	91.88±0.84**	81.10±0.74***	90.37±0.80***	77.88±0.84***	88.73±0.76***
54	73.23±0.75	51.45±1.08***	69.28±1.04***	41.12±0.87***	61.53±1.21***	35.58±1.07***	53.10±1.32***
55	46.52±0.77	26.22±0.86***	41.52±0.97***	19.38±1.00***	36.02±0.94***	12.53±1.00***	29.53±1.32***
56	18.37±0.63	11.77±0.59***	14.53±0.61**	9.95±0.53***	11.72±0.79	6.08±0.66***	8.42±0.62**

Table 1: Differences in the percentage of PCNA labeled cells in both digital and interdigital areas of the fore limb autopods of the tadpole developmental stages 53, 54, 55 and 56. Asterisks indicate the statistically significant differences (*** $P < 0.0001$, ** $P < 0.03$, * $P < 0.05$) versus each previous counting area. Digits are indicated as D1-4, while interdigits are indicated as ID1-4. Data are shown as mean ± SEM.
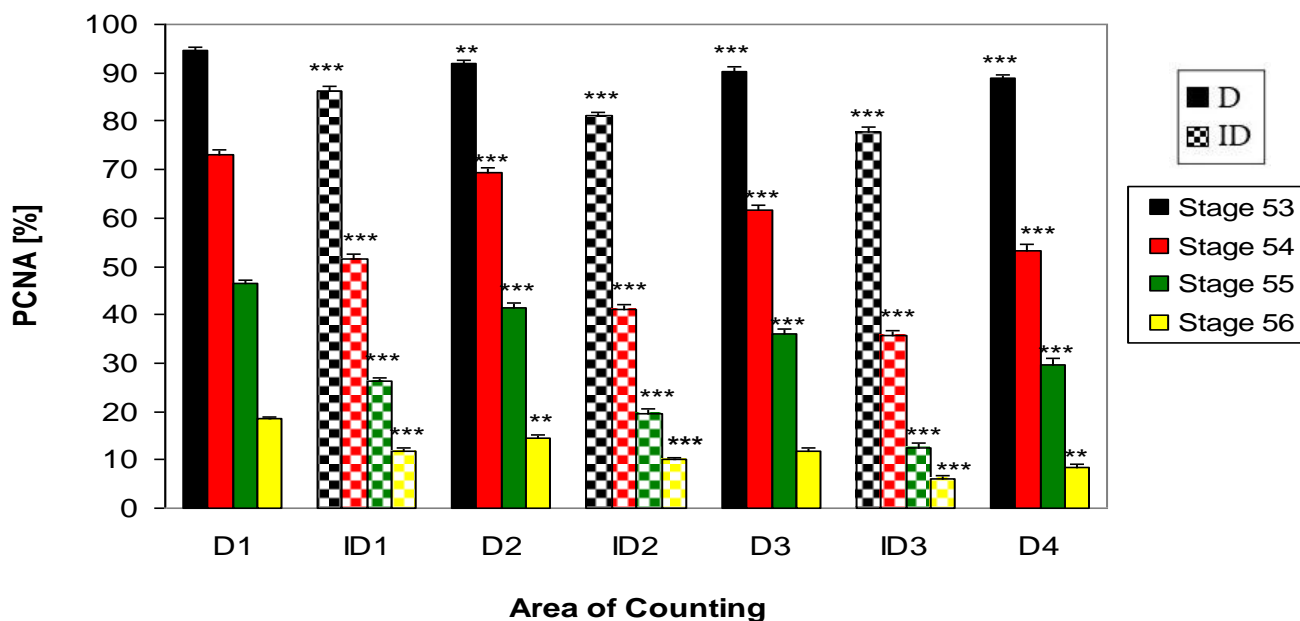

Fig.5: A histogram showing PCNA percentages (mitotic indices) (mean ± SEM) of both the digital and interdigital areas of the fore limb autopods of the tadpole developmental stages 53, 54, 55 and 56. Asterisks indicate the statistically significant differences (*** $P < 0.0001$, ** $P < 0.03$, * $P < 0.05$) versus each previous counting area. Digits are indicated as D1-4, while interdigits are indicated as ID1-4.
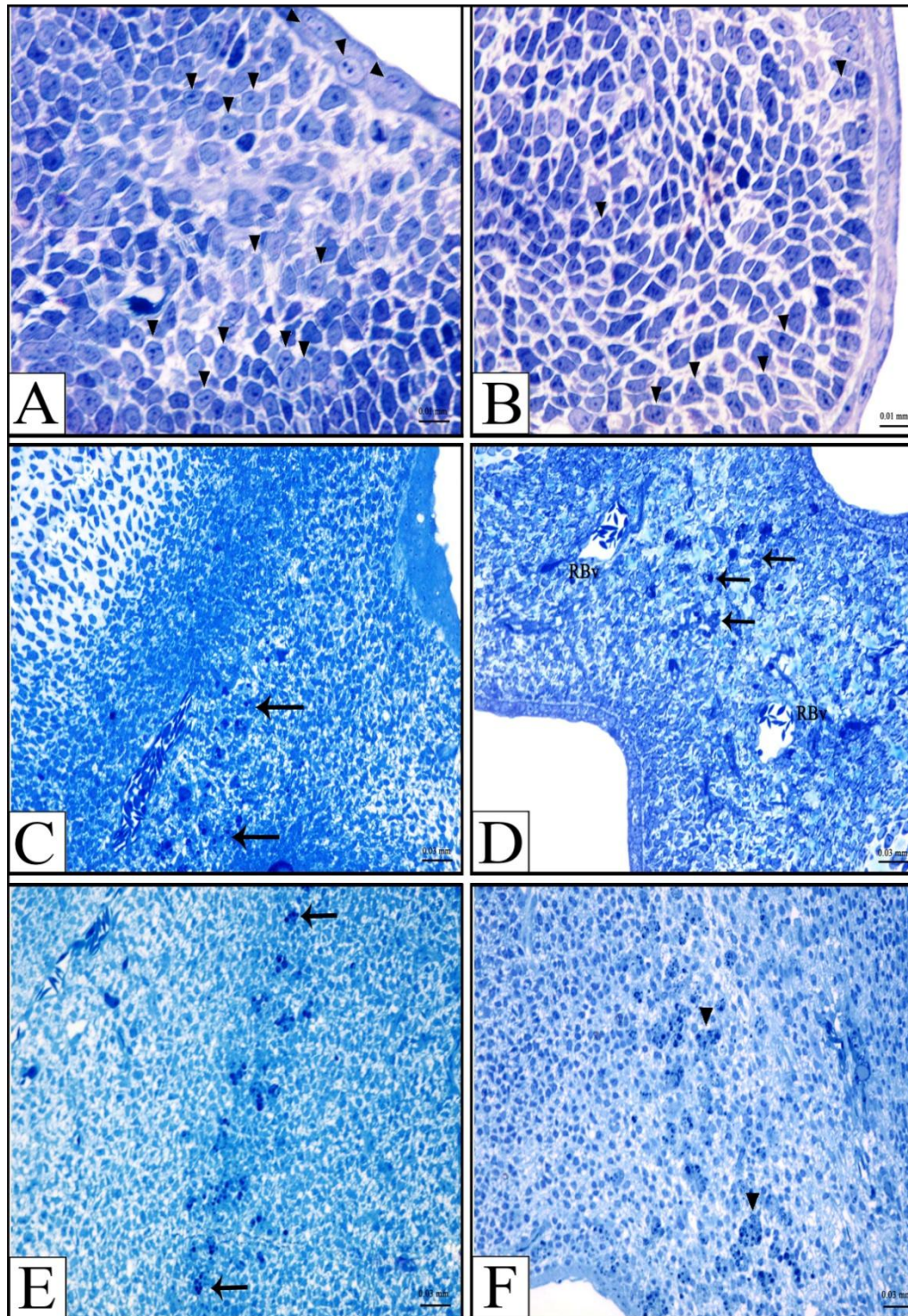
Fig. 6: Photomicrographs of representative longitudinal semithin histological sections through the autopod of fore limbs of the tadpole stage 53 (A) and 54 (B). Arrow heads point to the mitotic figures which were more abundant in the digital area than in the interdigital area. (C) through the autopod of the fore limbs of the chick developmental stage 31. (D&E) through the autopod of the hind limbs of the chick developmental stages 30 and 31, respectively. Arrows on E indicate the apoptotic cells in the third interdigital area of stage 31. (F) through the autopod of the hind limbs of the chick developmental stage 33. Arrow heads indicate the presence of macrophages with engulfed dead cells in the third interdigital area. All sections stained with Toluidine blue. Scale bar = 0.01 mm (A&B) and 0.03 mm (C,D,E&F).
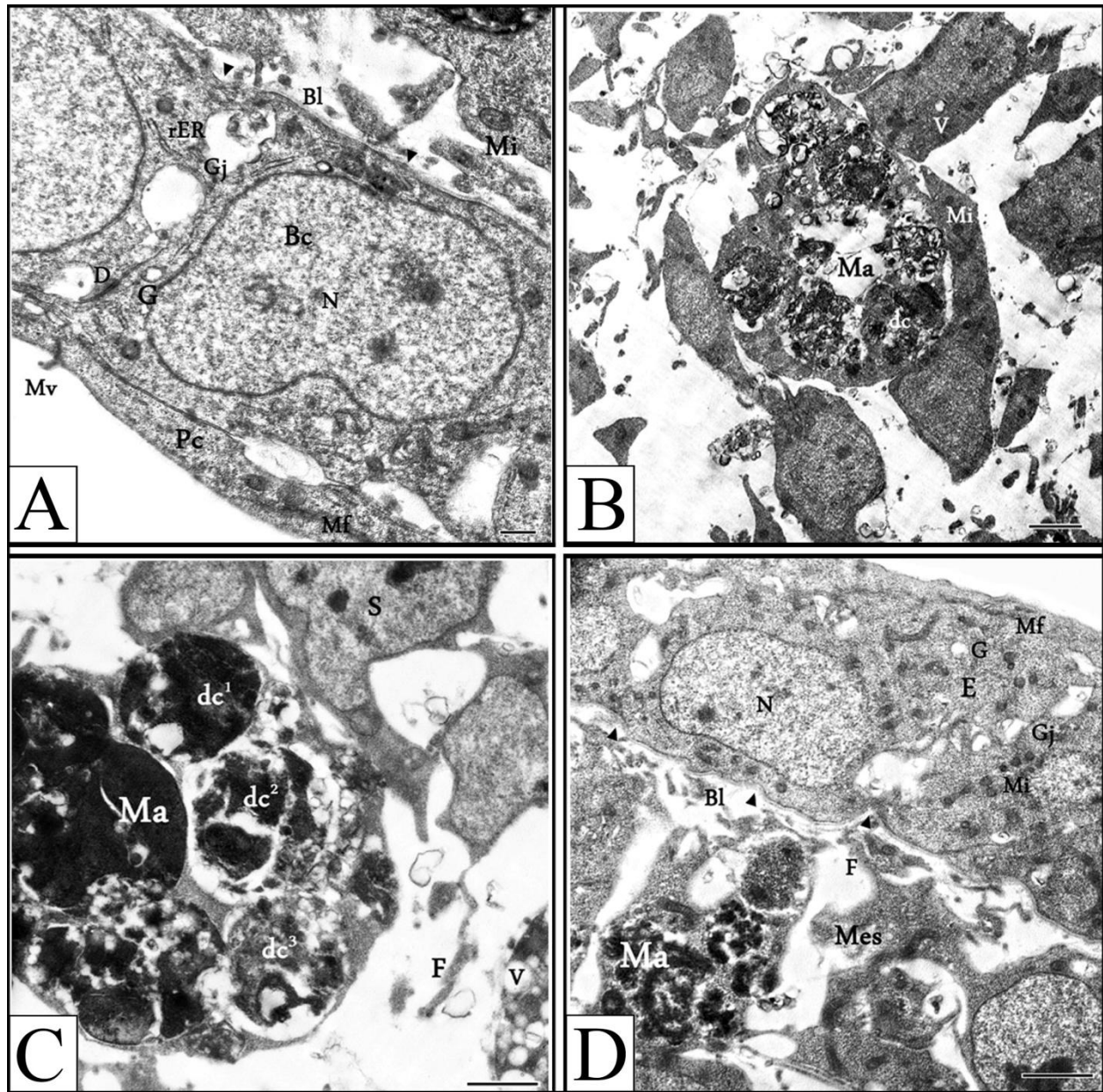
Fig. 7: Transmission electron micrographs (TEM) of the third interdigital area (A) and the second interdigital area (B) of stage 30 chick fore limb autopods showing Bl with discontinuities (arrow heads) (A) and Ma with a number of ingested dc (B). (C) through the third interdigital area of stage 31 showing mesenchyme cell death and Ma with dc. (D) through the second interdigital area of stage 32 showing the epithelial-mesenchyme interface, discontinuous Bl (arrow heads) and Ma. Scale bar = 500 nm (A) and 2μ (B-D).
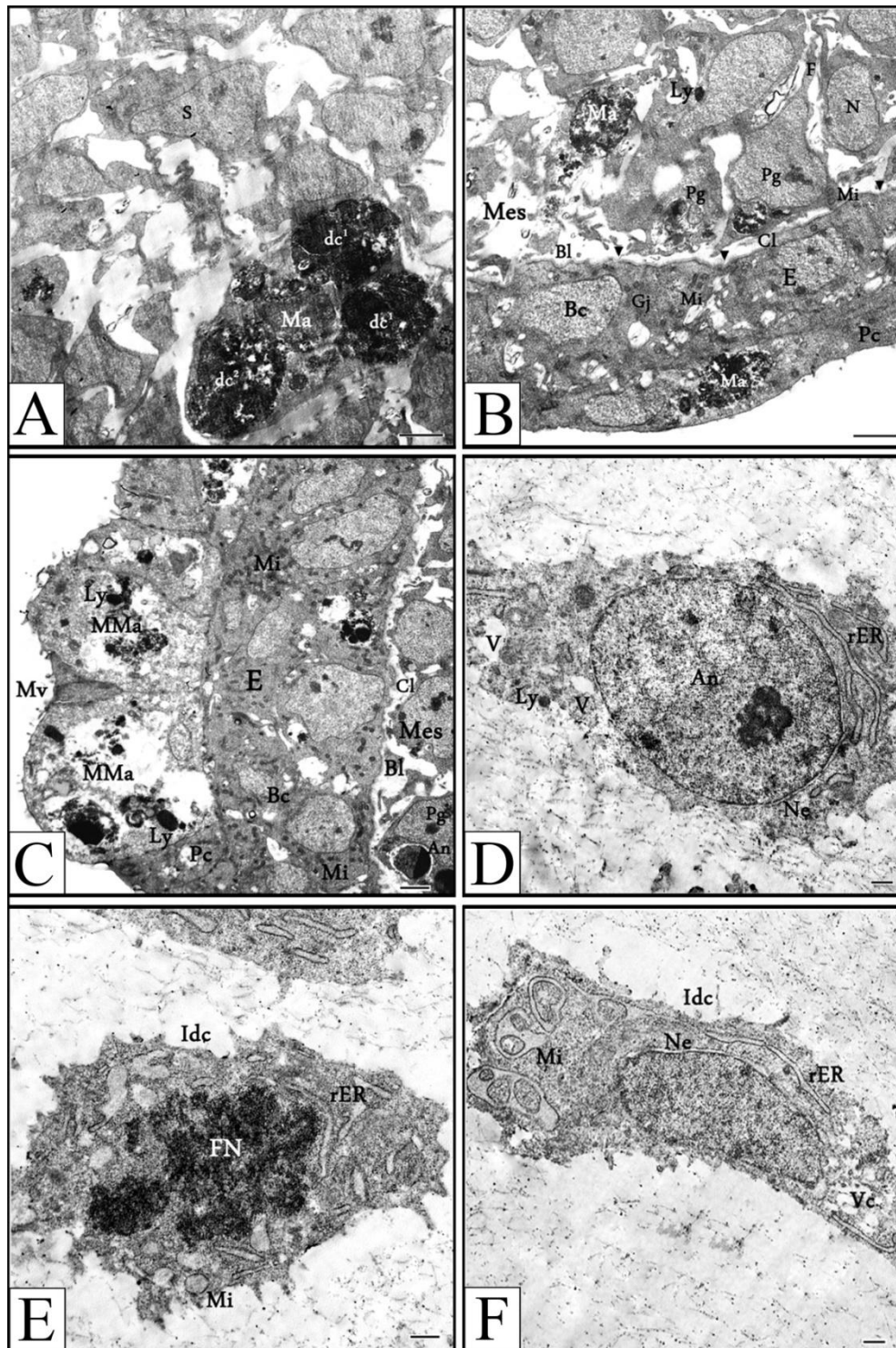
Fig. 8: TEM of the second interdigital area of stages 32 (A–C), 33 (D–F) chick fore limb autopods. (A) shows mesenchyme cell death and Ma with ingested dc. (B) shows epithelial-mesenchyme interface, the discontinuous Bl (arrow heads) and sublaminar Cl fibrils, Pg with a recently engulfed dc, mesenchyme cells with Ly, Pn and mesenchyme cell death. (C) shows epithelial-mesenchyme interface, sublaminar Cl, two MMa with Ly within the epithelium. (D–F) show isolated dead cells in the mesenchyme exhibiting different features of apoptosis, apoptotic nuclei with condensed chromatin along the periphery of the Ne, FN and distorted and degenerated cell organelles as well as the presence of Ly. Scale bar = 2μ (A–C) and 500 nm (D–F).
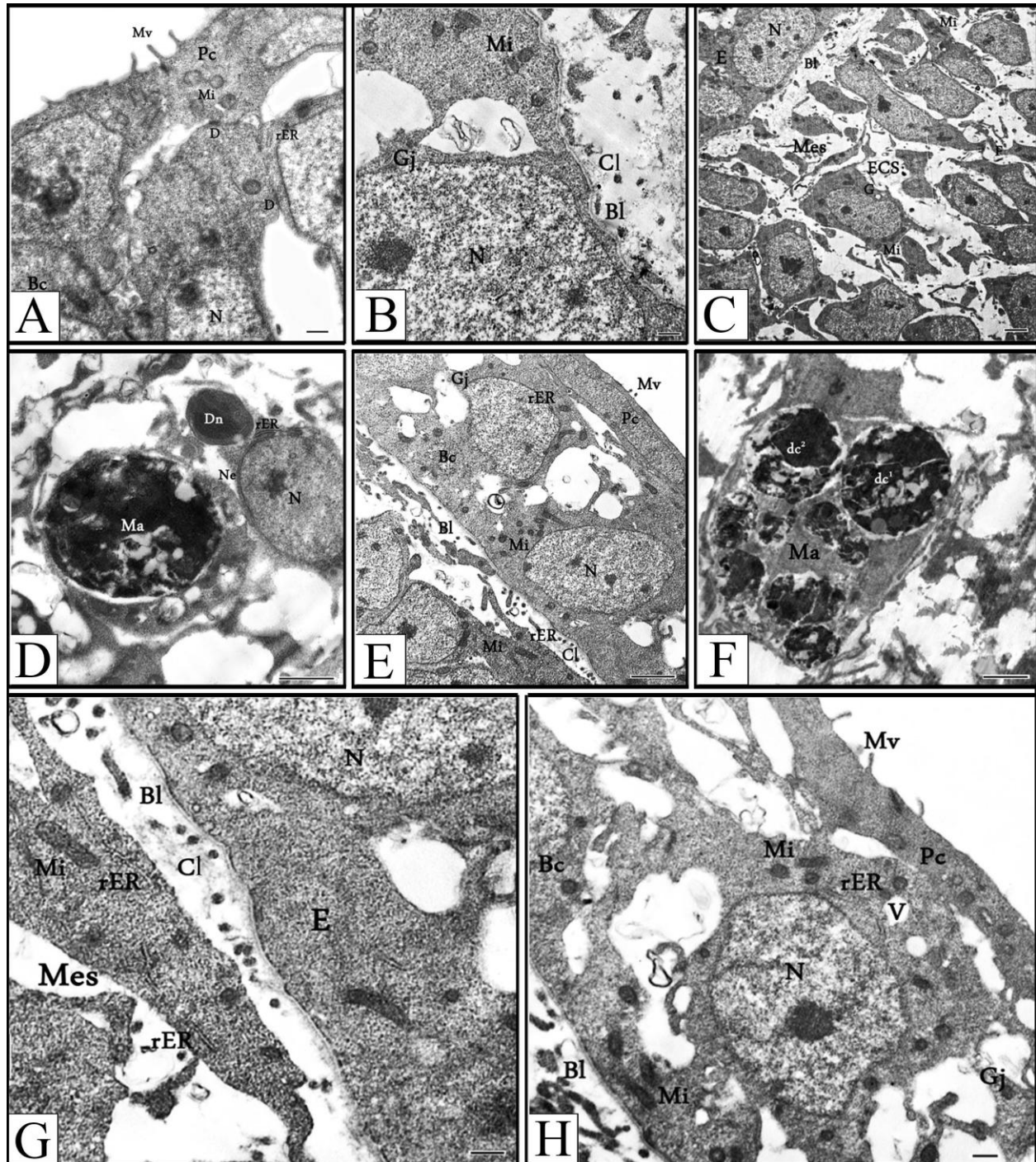
Fig. 9: TEM of the second interdigital area (A&B) and the third interdigital area (C&D) of stage 30, the first interdigital area of stage 31 (E&F) and the third interdigital area of stage 32 (G&H) chick hind limb autopods. (A) shows epithelium with Bc, Pc with Mv and well developed Mi and desmosomes. (B) shows epithelial-mesenchyme interface and sublaminar Cl. (C) shows epithelial-mesenchyme interface, stellate mesenchyme cells with extending filopodia and abundant Mi, continuous Bl in the digital area, large ECS in the interdigital area compared to its counterpart in the digital area (lower part). (D) shows Ma and a Dn during the process of phagocytosis. (E) shows epithelial-mesenchyme interface, Cl below the Bl. (F) shows different stages of dc associated with mesenchyme cell death. Scale bar = 500 nm (A,B,G&H), 2μ (C-F).
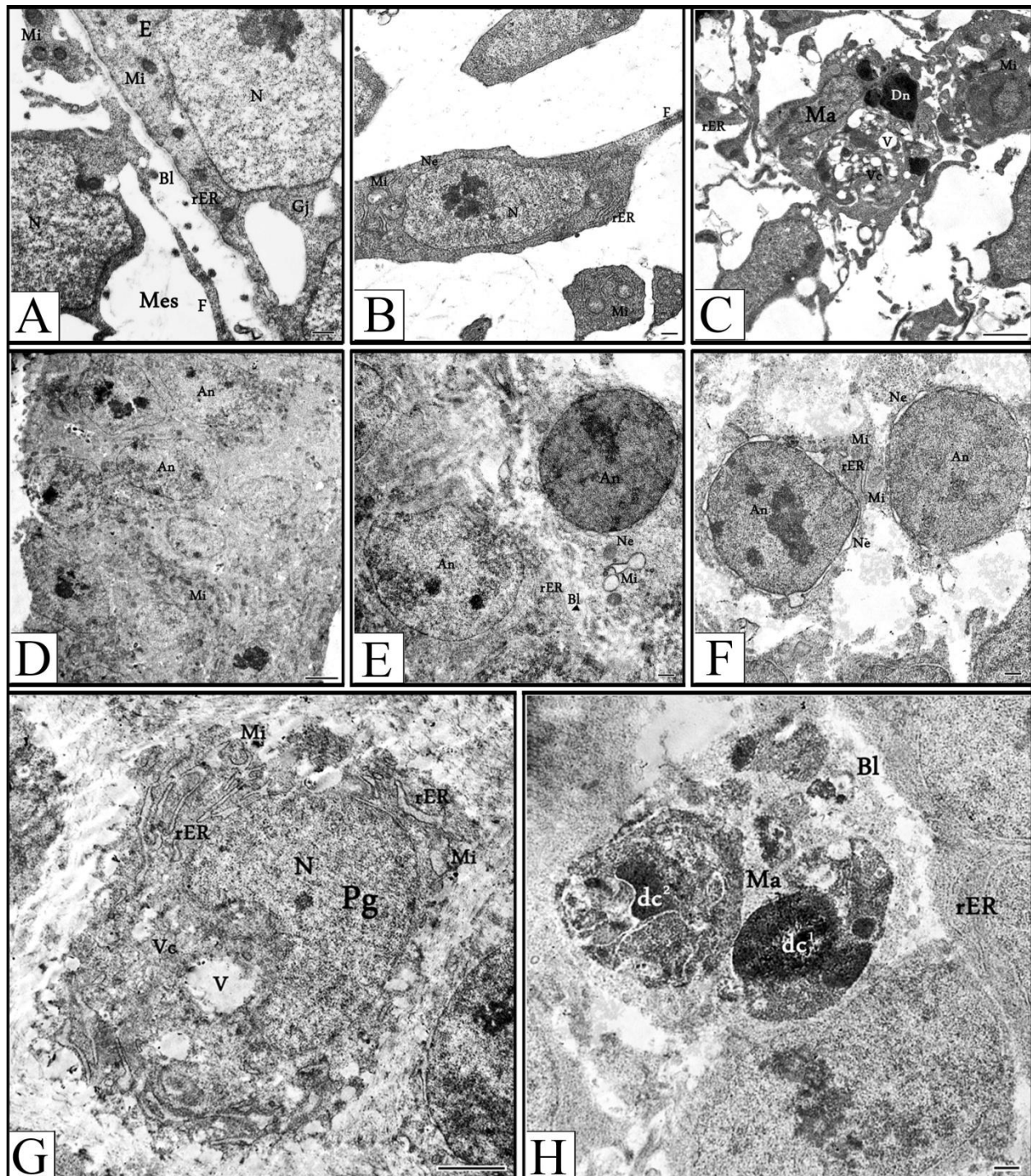
Fig. 10: TEM of the third interdigital area (A) and the first interdigital area (B&C) of stage 32, the third interdigital area of stage 33 (D–H) chick hind limb autopods. (A) shows epithelial-mesenchyme interface and discontinuous Bl. (B) shows a dead cell in the mesenchyme, distorted cell organelles and chromatin condensation. (C) shows Ma with partly digested contents and a Dn. (D) shows apoptotic nuclei and distorted cell organelles. (E) shows epithelial-mesenchyme interface, distorted Bl, swollen Mi and chromatin condensation. (F) shows apoptotic nuclei with dilated Ne, swollen Mi, dilated rER and chromatin condensation. (G) shows a Pg with kidney shaped nucleus, dilated rER, swollen Mi and Vc. (H) shows epithelial-mesenchyme interface showing a distorted Bl. Ma with ingested dc. Scale bar = 500 nm (A,B,E,F&H) and 2μ (C,D&G).

Abbreviations on the figures:
An, Apoptotic nucleus; Bc, Basal cell; Bl, Basal lamina; Cl, collagen; D, Desmosomes; dc, Dead cell; Dn, Degenerated nucleus; E, Epithelium; ECS, Extracellular space; En, Endothelum; F, Filopodia; FN, Fragmented nucleus; G, Golgi; Gj, Gap junction; Idc, Isolated dead cells; Ly, Lysosome; Ma, Macrophage; Mes, Mesenchyme; Mf, Microfilaments; Mi, Mitochondria; MMa, Mature macrophage; Mv, Micovilli; N, Nucleus; Ne, Nuclear envelope; Pc, Peridermal cell; Pg, Phagocyte; RBC, Red blood cell; rER, Rough endoplasmic reticulum; S, Stellate cell; V, Vacuole; Vc, Vacuolated cytoplasm.

Discussion

The outcome of the present study is in accordance with the study of Fallon and Cameron (1977) who stated that in spite of the fact that massive IPCD accompanies the formation of the free digits of birds (Dahn and Fallon, 2000), reptiles (Fallon and Cameron, 1977; Sorensen and Mesner, 2005) and mammals (Zakeri and Ahuja, 1994), it is important to note that it may not be the only mechanism accounting for the formation of the free digits. Cell death is not always an integral part of the mechanism of free digit formation, because in amphibians, it is absent (or nearly so) from the forelimbs of *Xenopus laevis*, *Bufo americanus*, *Ambystoma mexicanum*, *Ambystoma maculatum*, and *Taricha torosa* (Cameron and Fallon, 1977; Vlaskalin *et al*., 2004). An exception is provided by the presence of limited cell death positioned in the interdigits of limb buds of the urodele amphibian, the seepage salamander; but here it appears to have a relatively minor role as it flattens the interdigit web but does not free the digits (Franssen *et al*., 2005). Apart from this exception, and in accordance with the present results, it is generally accepted that individualization of amphibian digits appears to result from differential growth and elongation of the digits rather than by the apoptosis of the preformed interdigital tissue. In support of previous findings concerning the absence of cell death during the development of certain anuran autopod, all sections prepared from the tadpole specimens of the present study displayed negative immune-reaction with caspase-3 in a clear contrast to the situation in the chick embryos. This, somewhat, controversy in findings among different species called for investigating more amphibian species to resolve this issue.

In amphibians investigated so far and apart from the exception mentiond before, the progression of digit morphogenesis follows a specific pattern that differs from other tetrapods, where individual digits emerge sequentially from the limb plate during normal development but not regeneration (Vlaskalin *et al*., 2004). During the development of fore limb autopod in tadpoles, digits emerge from the limb plate in a sequential manner; digits IV and III are the first to grow out, followed by digits II and I. Determination of the rate of cell proliferation in the digital compared with the interdigital areas in the present study confirms that the digits emerge sequentially from the limb plate, especially that no apoptotic cells were detected in the interdigital area of the developing autopod of the toad. It has been reported that apoptotic cells can be easily recognized morphologically within a given histological section without applying specific stains (Chang *et al.,* 1998). This has been clearly confirmed in our results where apoptotic cells were darkly stained in the semithin sections stained with Toluidine blue. With regard to the mentioned exception, apoptosis in amphibians has been detected in one urodele in the presumptive interdigital tissues in both the fore limbs and the hind limbs (Franssen *et al*., 2005). At present, for anurans the only argument able to explain digit formation and the persistence of interdigital membranes in anurans was put forward by Cameron and Fallon (1977), but more amphibian species must be investigated to enhance our understanding of the cellular mechanisms involved in digit formation and its relationship to interdigital tissues (Goldberg and Fabrezi, 2008).

Another suggestion concerning digits formation came from Kelley (1970) who reported that cells may migrate from the interdigital area to the digital area as the digits become free. In an evident agreement with Kelley (1970), it can be suggested from the findings of the present study that the mesenchyme cells may migrate from the interdigital area to the digital area.

Further, using PCNA, this study demonstrated that the labeling index was higher in the prospective digital areas than in the interdigital areas starting from the tadpole developmental stage 53. As development proceeded, the labeling index displayed more gradual decrease in the interdigital areas compared with the digital areas. It is therefore proposed that free digits in the developing autopod of the

toad reach their specific morphogenesis, at least partly, as a result of a decrease in the proliferation rate of the interdigital area as compared to the digital area i.e. differential growth. Similarly, Cameron and Fallon (1977) proposed that free digits develop in *Xenopus laevis* fore limb as a result of a decrease in the proliferation rate of the interdigital areas as compared to the digital areas. Conversely, webbed digits develop in the hind limb as a result of an interdigital rate at least equal to the digital rate. It was proposed that differential growth of digital and interdigital areas occurs during digit individualization (Salas-Vidal *et al*., 2001; Hernández-Martínez *et al*., 2009). This suggests that the role of IPCD is the control of growth of the interdigital area and thus allows digits to protrude distally (Hernández-Martínez and Covarrubias, 2011). It has also been reported that the epithelium of the interdigital area might also play an active role in the formation of digits (Kelley, 1973). Another evidence of a mutual dependence between the regressive changes in the mesenchymal and ectodermal components of the interdigital area was introduced by Hurlé and Fernández-Terán, (1984). Although, interdigital mesenchyme cell death and disruption of the ectodermal tissue have been reported as the main mechanisms accounting for the disappearance of the interdigital tissue (Hurlé *et al*., 1995), the mechanism of interdigital tissue regression cannot be explained by a simplistic spontaneous disintegration of the tissue.

PCD is considered one of the most important cellular processes in the morphogenesis of organs and tissues during animal development as it plays a key role in eliminating unnecessary cells to achieve complicated histogenesis. During limb development, all amniote embryos exhibit massive PCD at the level of the interdigital tissue, and this has been considered responsible for sculpturing the digits from the early hand or foot plate (Montero and Hurlé, 2010). Physiological PCD has been proposed to occur by apoptosis following two main pathways depending on the origin of the death stimulus, cytochrome C liberation from the mitochondria (intrinsic or mitochondrial pathway) or activation of death receptors (extrinsic pathway) (Boatright and Salvesen, 2003; Zuzarte-Luís *et al*., 2006). Such pathways converge in the activation of cysteine proteases known as caspases, which execute the cell death programme, leading to typical apoptotic changes within the cell. It would therefore be expected that caspases loss of function experiments could cause inhibition of IPCD, promoting syndactyly phenotypes (Montero and Hurlé, 2010). The intrinsic pathway involves the participation of mitochondria, which release caspase-activating proteins into the cytosol, thereby triggering apoptosis (Green and Reed, 1998). The mitochondria of the interdigital area in the present study appeared distorted and this mitochondrial damage demonstrates the intrinsic pathway of caspase action. However, demonstration of the involvement of the death receptors i.e. the extrinsic pathway is out of the scope of the present study.

The areas of IPCD are found between the developing digits of all amniote embryos (Hurlé *et al*., 1995). According to the present study, apoptotic cells were positively demonstrated in the interdigital mesenchyme by caspase-3 in case of the developing chick autopod but there was no trace of these apoptotic cells in its tadpole counterpart using the same immunohistochemical technique. Furthermore, investigating the ultrastructural changes in the interdigital area within the developing chick autopod revealed the presence of different stages of apoptosis. Similarly, apoptosis has been observed in the interdigital area of many tetrapod species (Chang *et al*, 1998; Chen and Zhao, 1998; Sato *et al*., 2010).

The amniote limb is a classic model for studying the mechanisms that control PCD during embryogenesis (Hurlé, 1988), with the majority of the descriptive and experimental work performed in chick limbs. PCD in the interdigital area of the developing limb is a classical example of morphogenetic cell death and it has been reported that the loss of interdigital cells is a paradigm of cell death during autopod development (Chautan *et al*., 1999). Across species, different patterns of PCD correlate with different morphologies of the interdigital area, and thus the temporal and spatial distribution of IPCD is closely related to the morphogenesis of digits (Merino *et al*., 1999; Fernández-Terán *et al*., 2006). For example, PCD inhibition correlates with survival of interdigital webbing (Hurlé *et al*., 1996). Thus, in species with free digits such as the chick, mouse or human, the PCD extend through the entire interdigital mesoderm (Hurlé *et al*., 1996). However, in species with webbed or partially free digits such as the duck (Gañan *et al*., 1998), Turtle (Fallon and Cameron, 1977), and bat (Weatherbee *et al*., 2006), the PCD is less abundant and restricted to the distal part of the interdigital areas.

The results of the present study showed that the IPCD is an integral part of the formation of free digits in the chick embryo, while it is never a part of free digit formation in the toad *Bufo regularis*. In the latter, cell migration and differential growth are the alternative processes through which digits can be freed. The high cellular condensation in the interdigital areas in the early tadpole developmental stage, *i.e.* 53 compared with the successive stages pointed to the possibility of cell migration during the development of autopod in the toad *Bufo regularis*. It can therefore be postulated that besides differential growth which includes more active cell division in the digital area than in the interdigital area in the developing autopod of the toad, cell migration plays an important role during morphogenesis. It can be therefore concluded that in the developing autopod of the tadpoles, digits appear sequentially as outgrowths from the limb plate. It can also be postulated that cell migration in case of the developing chick autopod is comparatively limited owing to the presence of apoptosis which is evidently absent in the developing autopod of toad. Investigating the process of cell migration during the formation of digits needs special techniques and is therefore out of the scope of this study. Although cell migration is a complex process, live imaging and genetic approaches are yielding much information in terms of morphogenetic development (Aman and Piotrowski, 2010).

In accordance with the study of Hurlé and Fernández-Terán (1983) on the ultrastructure of the regressing interrdigital areas of the chick foot, three main morphological features in the regressing interdigital areas were involved in the tissue disappearance: 1) mesenchymal cell death; 2) deposition of collagenous material in the epithelial-mesenchyme interface accompanied by rupture of the ectodermal basal lamina; and 3) detachment of the ectodermal tissue into the amniotic sac. An epithelial-mesenchyme interaction during digit separation was strongly suggested by the latter study and others (Fernández-Terán *et al*., 2013).

The epithelial-mesenchyme interaction plays an integral role in the morphogenesis of vertebrate limbs but remains a controversial and complex problem involving cell surfaces and extracellular matrices. The importance of the epithelial-mesenchyme interface in relation to the growth of the limb buds has motivated several studies of the ectoderm-basal lamina-mesenchyme complex in different vertebrates (Gumpel-Pinot, 1981; Al-Mukhaini *et al*., 2012). Both the ectodermal and mesenchymal tissues are separated by an interface of extracellular material which is a critical element in the interaction process (Hay, 1981; Fernández-Terán *et al*., 2013). The characteristics of these extracellular matrix components can modify the differentiation of the epithelium and the behaviour of the underlying mesenchymal tissue. The most conspicuous changes in the extracellular matrix were disruptions of the ectodermal basal lamina and an intense deposition of collagenous material under the marginal ectoderm. In addition, mesenchymal macrophages appeared to migrate through the epithelial tissue to be detached into the amniotic sac. Modifications of the basal lamina of regressing epithelial structures might play a role in the disappearance of the tissue. The degree of basal lamina discontinuity seen in the present study depended on the mesenchyme cell degeneration.

In line with other previous transmission electron microscopy studies, the present results have shown that PCD in the interdigital mesoderm follows a morphological pattern of apoptosis (García-Martinez *et al*., 1993; Mori *et al*., 1995). Most interdigital dying cells appeared rounded and electron dense with the nucleus exhibiting a characteristic peripheral condensation of the chromatin. Vacuolation of most of the cytoplasmic organelles and the presence of lysosomes were evident. The most prominent feature was the presence of distorted and swollen mitochondria within the interdigital areas of the developing autopod. The apoptotic cells underwent fragmentation and the fragments resulting from this process appeared as darkly stained spherules which usually contained a small nuclear fragment. The resulting debris was removed by phagocytosis. Removal was performed both by the neighboring healthy mesenchyme cells and by incoming macrophages (Hurlé *et al*., 1996; Montero and Hurlé, 2010).

The origin of the phagocytic cells is a controversial question. Early phagocytes containing only one or two engulfed dead cells are morphologically indistinguishable from limb mesenchymal cells. This suggests that, as described in other embryonic areas of cell death (García-Porrero *et al*., 1984) healthy limb mesenchymal cells become poised to remove dying cells by phagocytosis. However, experiments by Cuadros *et al*. (1992) using chick-quail chimeras suggested that at least part of the phagocytic cells

present in the areas of cell death of the developing limb are specialized macrophages of hemopoietic origin. This last possibility is strongly supported by other studies using specific immunolabeling for macrophages (Hopkinson-Woolley *et al*., 1994).

The intercellular communication is important in the determination of pattern during morphogenesis and the elucidation of structural mechanisms which mediate intercellular communication between cells of the limb is fundamental during development. Gap junctions are one of the most important membrane specializations that have been noted in the developing chick limb autopod (Kelley and Fallon, 1978). Cell to cell communication through Gap junctions allows the translocation of ions, metabolites and second messengers from cell to cell, which is essential for cellular functions such as cell growth, proliferation and differentiation (Ross and Pawlina, 2005).

Based on the present findings, it can be concluded that the observed differences in the mode of autopod morphogenesis in the developing toad and chick point to fundamentally different mechanisms in both models. This in turn, called for reconsidering the generally accepted concept which says that the tetrapod limb follows a conservative developmental pattern (Gardiner, *et al.,*1998; Mabee, 2000; Hinchliffe, 2002).

REFERENCES

Al-Mukhaini, N.; Ba-Omar, T. and Mahmoud, I. (2012): Ultrastructural study of limb bud development in green turtles *Chelonia mydas*. Asian Herpetol. Res., 3: 69–78.

Aman, A. and Piotrowski, T. (2010): Cell migration during morphogenesis. Dev. Biol., 341: 20–33.

Boatright, K. and Salvesen, G. (2003): Mechanisms of caspase activation. Curr. Opin. Cell Biol., 15: 725–731.

Badawy, G.; Sakr S. and Atallah, M. (2012): Comparative study of the skeletogenesis of limb autopods in the developing chick *Gallus domesticus* and toad *Bufo regularis*. RJPBCS, 3: 966–988.

Bratton, S.; MacFarlane, M.; Cain, K. and Cohen, G. (2000): Protein complexes activate distinct caspase cascades in death receptor and stress-induced apoptosis. Exp. Cell Res., 256: 27–33.

Cameron, J. and Fallon, J. (1977): The absence of cell death during development of free digits in amphibians. Dev. Biol., 55: 331–338.

Chang, H.; Tse, Y. and Kaufman, M. (1998): Analysis of interdigital spaces during mouse limb development at intervals following amniotic sac puncture. J. Anat., 192: 59–72.

Chautan, M.; Chazal, G.; Cecconi, F.; Gruss, P. and Golstein, P. (1999): Interdigital cell death can occur through a necrotic and caspase-independent pathway. Curr. Biol., 9: 967–970.

Chen, Y. and Zhao, X. (1998): Shaping limbs by apoptosis. J. Exp. Zool., 282: 691–702.

Cuadros, M.; Coltey, P.; Nieto, C. and Martin, C. (1992): Demonstration of a phagocytic cell system belonging to the hemopoietic lineage and originating from the yolk sac in the early avian embryo. Development, 115: 157–168.

Dahn, R. and Fallon, J. (2000): Interdigital regulation of digit identity and homeotic transformation by modulated BMP signaling. Science, 289: 438–441.

Elmore, S. (2007): Apoptosis: a review of programmed cell death. Toxicol. Pathol., 35: 495–516.

Fallon, J. and Cameron, J. (1977): Interdigital cell death during limb development of the turtle and lizard with an interpretation of evolutionary significance. J. Embryol. Exp. Morphol., 40: 285–289.

Fernández-Terán, M.; Hinchliffe, J. and Ros, M. (2006): Birth and death of cells in limb development: a mapping study. Dev. Dyn., 235: 2521–2537.

Fernández-Terán, M.; Ros, M. and Mariani, F. (2013): Evidence that the limb bud ectoderm is required for survival of the underlying mesoderm**.** Dev. Biol., 15:341–352.

Franssen, A.; Marks, S.; Wake, D. and Shubin, N. (2005): Limb chondrogenesis of the seepage salamander, *Desmognathus aeneus* (*amphibia: plethodontidae*). J. Morphol., 265: 87–101.

Gañan, Y.; Macías, D.; Basco, R.; Merino, R. and Hurlé, J. (1998): Morphological diversity of the avian foot is related with the pattern of msx gene expression in the developing autopod. Dev. Biol., 196: 33–41.

García-Martinez, V.; Macías, D.; Gañan, Y.; García-Lobo, J.; Francia, M.; Fernández-Terán, M. and Hurlé, J. (1993): Internucleosomal DNA fragmentation and programmed cell death in a zone of prospective necrosis from the chick wing bud. J. Cell Sci., 106: 201–208.

García-Porrero, J.; Colvée, E. and Ojeda, J. (1984): Cell death in the dorsal part of the chick optic cup, evidence for a new necrotic area. J. Embryol. Exp. Morph., 80: 241–249.

Gardiner, D.; Torok, M.; Mullen, L. and Bryant, S. (1998): Evolution of vertebrate limbs: robust morphology and flexible development. Amer. Zool., 38: 659–671.

Goldberg, J. and Fabrezi, M. (2008): Development and variation of the anuran webbed feet (*Amphibia, Anura*). Zool. J. Linn. Soc., 152: 39–58.

Green, D. and Reed, J. (1998): Mitochondria and apoptosis. Science, 281: 1309–1312.

Gumpel-Pinot, M. (1981): Ectoderm-mesoderm interactions in relation to limb-bud chondrogenesis in the chick embryo: transfilter cultures and ultrastructural studies. J. Embryol. Exp. Morph., 65: 73–78.

Hamburger, V. and Hamilton, H. (1951): A series of normal stages in the development of the chick embryo. J. Morphol., 88: 49–92.

Hay, E. (1981): Collagen and embryonic development. In Hay, E. (ed.) Cell biology of extracellular matrix. New York: Plenum Press, pp. 379–409.

Hernández-Martínez, R. and Covarrubias, L. (2011): Interdigital cell death function and regulation: new insights on an old programmed cell death model. Dev. Growth Differ., 53: 245–258.

Hernández-Martínez, R.; Castro-Obregón, S. and Covarrubias, L. (2009): Progressive interdigital cell death: regulation by the antagonistic interaction between fibroblast growth factor 8 and retinoic acid. Development, 136: 3669–3678.

Hinchliffe, J. (1982): Cell death in vertebrate limb morphogenesis. In: Harrison, R. and Navatnaram, V. (eds.) Progress in anatomy. Cambridge: Cambridge University Press, p. 1–19.

Hinchliffe, J. (2002): Developmental basis of limb evolution. Int. J. Dev. Biol., 46: 835–845.

Hinchliffe, J. and Thorogood, P. (1974): Genetic inhibition of mesenchymal cell death and development of form and skeletal pattern in the limb of *talpid3* (*ta3*) mutant chick embryos. J. Embryol. Morphol., 87: 163–174.

Hopkinson-Woolley, J.; Hughes, D.; Gordon, S. and Martin, P. (1994): Macrophage recruitment during limb development and wound healing in the embryonic and foetal mouse. J. Cell Sci., 107: 1159–1167.

Huang, C. and Hales, B. (2002): Role of caspases in murine limb bud cell death induced by 4-hydroperoxycyclophosphamide, an activated analog of cyclophosphamide. Teratology, 66: 288–299.

Hurlé, J. (1988): Cell death in developing systems. Meth. Achiev. Exp. Pathol. 13: 55–86.

Hurlé, J. and Fernández-Terán, M. (1983): Fine structure of the regressing interdigital membranes during the formation of the digits of the chick embryo leg bud. J. Embryol. Exp. Morph., 78: 195–209.

Hurlé, J. and Fernández-Terán, M. (1984): Fine structure of the interdigital membranes during the morphogenesis of the digits of the webbed foot of the duck embryo. J. Embryol. Exp. Morph., 79: 201–210.

Hurlé, J.; Ros, M.; García-Martinez, V.; Macías, D. and Gañan, Y. (1995): Cell death in the embryonic developing limb. Scan. Microsc., 9: 519–534.

Hurlé, J.; Ros, M.; Climent, V. and García-Martinez, V. (1996): Morphology and significance of programmed cell death in the developing limb bud of the vertebrate embryo. Microsc. Res. Tech., 34: 236–246.

Jacobson, M.; Weil, M. and Raff, M. (1997): Programmed cell death in animal development. Cell, 88: 347–354.

Karnovsky, M. (1965): A formaldehyde-glutraldehyde fixative of high osmolarity for use in electron microscopy. J. Cell Biol., 27: 137–138.

Kelley, R. (1970): An electron microscopic study of mesenchyme during development of interdigital spaces in man. Anat. Rec., 168: 43–53.

Kelley, R. (1973): Fine structure of the apical rim-mesenchyme complex during limb morphogenesis in man. J. Embryol. Exp. Morph., 29: 117–131.

Kelley, R. and Fallon, J. (1978): Identification and distribution of gap junctions in the mesoderm of the developing chick limb bud. J. Embryol. Exp. Morph., 46: 99–110.

Korn, M. and Cramer, K. (2007): Windowing chicken eggs for developmental studies. J. Vis. Exp., 8: 306.

Kurki, P.; Ogata, K. and Tan, E. (1988): Monoclonal antibodies to proliferating cell nuclear antigen (PCNA)/cyclin as probes for proliferating cells by immunofluorescence microscopy and flow cytometry. J. Immunol. Meth., 109: 49–59.

Mabee, P. (2000): Developmental data and phylogenetic systematics: evolution of the vertebrate limb. Amer. Zool., 40: 789–800.

Maghsoudi, V.; Zakeri, Z. and Lockshin, R. (2012): Programmed cell death and apoptosis - where it came from and where it is going: from Elie Metchnikoff to the control of caspases. Exp. Oncol., 34: 146–152.

Merino, R.; Gañan, Y.; Macías, D.; Rodríguez-León, J. and Hurlé, J. (1999): Bone morphogenetic proteins regulate interdigital cell death in the avian embryo. Ann. N Y Acad. Sci., 887: 120–132.

Milaire, J. (1977): Histochemical expression of morphogenetic gradients during limb morphogenesis (with particular reference to mammalian embryos). Birth Defects Orig. Artic. Ser., 13: 37–67.

Milligan, C.; Prevette, D.; Yaginuma, H.; Homma, S.; Cardwell, C.; Fritz, L.; Tomaselli, K.; Oppenheim, R. and Schwartz, L. (1995): Peptide inhibitors of the ICE protease family arrest programmed cell death of motoneurons *in vivo* and *in vitro*. Neuron, 15: 385–393.

Montero, J. and Hurlé, J. (2010): Sculpturing digit shape by cell death. Apoptosis, 15: 365–375.

Mori, C.; Nakamura, N.; Kimura, S.; Irie, H.; Takigawa, T. and Shiota, K. (1995): Programmed cell death in the interdigital tissue of the fetal mouse limb is apoptosis with DNA fragmentation. Anat. Rec., 242: 103–110.

Ross, M. and Pawlina, W. (2005): Histology: a text and atlas with correlated cell and molecular biology (5th edn). USA: Lippincott Williams & Wilkins.

Salas-Vidal, E.; Valencia, C. and Covarrubias, L. (2001): Differential tissue growth and patterns of cell death in mouse limb autopod morphogenesis. Dev. Dyn., 220: 295–306.

Sato, K.; Seki, R.; Noro, M.; Yokoyama, H. and Tamura, K. (2010): Morphogenetic change of the limb bud in the hand plate formation. J. Exp. Zool. (Mol. Dev. Evol.), 314B: 539–551.

Saunders, J. and Fallon, J. (1966): Cell death in morphogenesis. In Locke, M. (ed.) Major Problems in Developmental Biology. New York: Academic Press, 289–314.

Saunders, J.; Gasseling, M. and Saunders, L. (1962): Cellular cell death in morphogenesis of the avian wing. Dev. Biol., 5: 147–178.

Sedra, S. and Michael, M. (1961): Normal table of the Egyptian toad, *Bufo regularis* Reuss, with an addendum of the standardization of the stages considered in previous publications. Cesk. Morf., 9: 333–351.

Shou, S.; Carlson, H. Perez, W. and Stadler, S. (2013): HOXA13 regulates Aldh1a2 expression in the autopod to facilitate interdigital programmed cell death. Dev. Dyn., 242: 687-698.

Sorensen, E. and Mesner, P. (2005): IgH-2 cells: a reptilian model for apoptotic studies. Comp. Biochem. Physiol. (Biochem. Mol. Biol.), 140B: 163–170.

Steller, H. (1995): Mechanisms and genes of cellular suicide. Science, 267: 1445–1449.

Sternberger, L. (1979): The unlabelled antibody peroxidase-antiperoxidase (PAP) method. In: Cohen, S. and McClusky, R. (eds.) Immunocytochemistry. (2nd edn). New York: John Wiley and sons, 104–169.

Tousson, E.; Ali, E.; Ibrahim, W. and Mansour, M. (2011): Proliferating cell nuclear antigen as a molecular biomarker for spermatogenesis in PTU-induced hypothyroidism of rats. Reprod. Sci.,18:679–686.

Umpierre, C.; Little, S. and Mirkes, P. (2001): Co-localization of active caspase-3 and DNA fragmentation (TUNEL) in normal and hyperthermia-induced abnormal mouse development. Teratology, 63: 134–143.

Van Dierendonck, J.; Wijsman, J.; Keijzer, R.; van de Velde, C. and Cornelisse, C. (1991): Cell-cycle-related staining patterns of anti-proliferating cell nuclear antigen monoclonal antibodies. Comparison with BrdU labeling and Ki67 staining. Am. J. Pathol., 138: 1165–1172.

Vlaskalin, T.; Wong, C. and Tsilfidis, C. (2004): Growth and apoptosis during larval forelimb development and adult forelimb regeneration in the newt (*Notophthalmus viridescens*). Dev. Genes. Evol., 214: 423–431.

Weatherbee, S.; Behringer, R.; Rasweiler, J. and Niswander, L. (2006): Interdigital webbing retention in bat wings illustrates genetic changes underlying amniote limb diversification. PNAS, 103: 15103–15107.

Zakeri, Z. and Ahuja, H. (1994): Apoptotic cell death in the limb and its relationship to pattern formation. Biochem. Cell Biol., 72: 603–613.

Zuzarte-Luís, V.; Berciano, M.; Lafarga, M. and Hurlé, J. (2006): Caspase redundancy and release of mitochondrial apoptotic factors characterize interdigital apoptosis. Apoptosis, 11: 701–715.